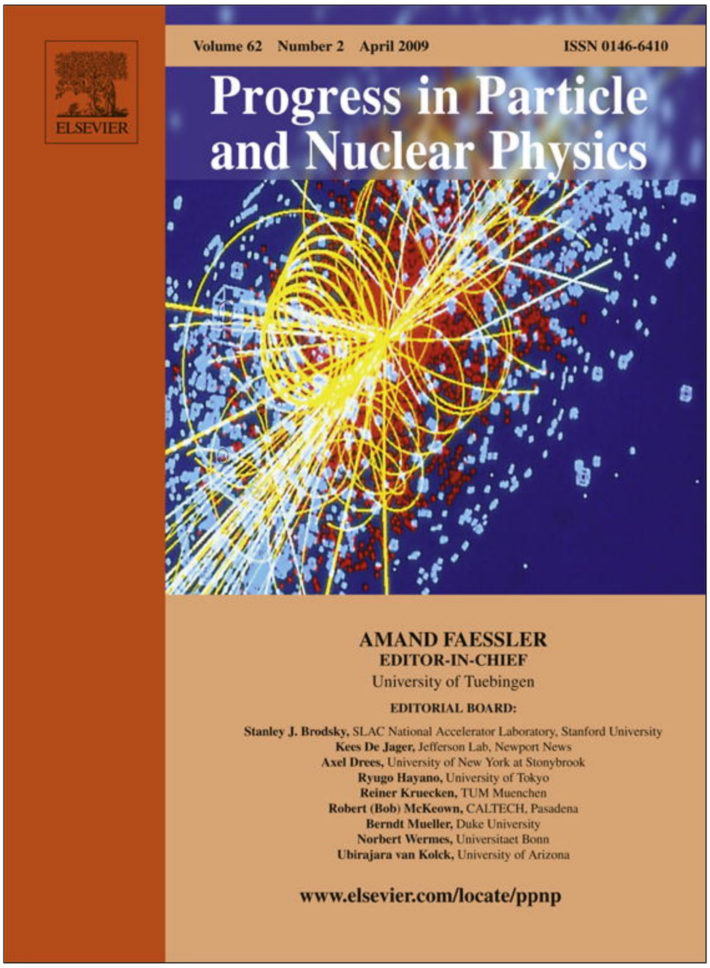
ELSEVIER
Volume 62 Number 2 April 2009
ISSN 0146-6410
Progress in Particle and Nuclear Physics
AMAND FAESSLER
EDITOR-IN-CHIEF
University of Tuebingen
EDITORIAL BOARD:
Stanley J. Brodsky, SLAC National Accelerator Laboratory, Stanford University
Kees De Jager, Jefferson Lab, Newport News
Axel Drees, University of New York at Stonybrook
Ryugo Hayano, University of Tokyo
Reiner Kruecken, TUM Muenchen
Robert (Bob) McKeown, CALTECH, Pasadena
Berndt Mueller, Duke University
Norbert Wermes, Universitaet Bonn
Ubirajara van Kolck, University of Arizona
www.elsevier.com/locate/ppnp

Progress in Particle and Nuclear Physics 62 (2009) 445–450

Contents lists available at ScienceDirect

Progress in Particle and Nuclear Physics

journal homepage: www.elsevier.com/locate/ppnp

Review

Probing dense baryonic matter with strangeness

N. Herrmann, (FOPI collaboration)

Ruprecht-Karls Universität Heidelberg, Germany

ARTICLE INFO

Keywords:
Dense baryonic matter
Strangeness
Nucleus–nucleus collision
Multi-baryonic strange bound states
Heavy-ion interactions

ABSTRACT

Strange particles allow to probe the properties of hot and dense baryonic matter. At incident energies close to the production threshold medium effects on the strange hadrons are magnified. Available data on $K^{0,+,-}K^*$ (892), Φ, Λ, and Σ^* (1385) are summarized for the system Al + Al at an incident energy of 1.9 AGeV and compared to statistical model calculations. Results of searches for multi-baryonic strange bound states in the Λp-channel are presented.

1. Introduction

Modifications of hadron properties in dense baryonic matter are a current subject of intensive research in hadron physics. Various theoretical approaches [1–3] agree qualitatively on predicting, for example, modifications of masses and coupling constants for kaons and anti-kaons. Due to the density dependence of the KN ($\overline{K}$N) potential, the K^- effective mass is expected to drop, whereas the mass of K^+ mesons is predicted to rise with increasing density of nuclear matter. Already two decades ago, Kaplan and Nelson [4] pointed out that due to additional attractive interactions with the surrounding nucleons a condensation of anti-kaons (K^-) may take place in a dense baryonic environment as encountered in the interior of neutron stars.

In nucleus–nucleus collisions the formation of dense K^- meson clusters is nowadays being searched for. Kaons (K^+, K^0), on the other hand, have a relatively long mean free path in the nuclear matter at low momenta. Therefore they are a good probe for studying the in-medium properties of hadrons produced in collisions between nuclei at energies close to the respective nucleon–nucleon production thresholds [5]. However, for a quantitative understanding of strangeness production in such collisions the knowledge of the elementary production cross-sections at finite baryonic densities is essential.

2. Kaon production in $\pi + A$ reactions

In order to examine the Kaon interaction at normal nuclear matter density, a measurement of K^0_S – mesons in π^- – nucleus interaction was undertaken with the FOPI detector at SIS18 of GSI. A pion beam has the advantage that relatively little momentum is brought into the system, so that possible medium effects are maximized. Details about the experimental conditions can be found in [6].

To shed light on the in-medium effects on the K^0 production at $\rho \leq \rho_0$, the K^0 inclusive cross-section is compared to the one in vacuum and to model predictions at finite densities. To obtain an inclusive vacuum cross-section, all exclusive channels ($\pi^- + p \to K^0\,\Sigma^0, \pi^- + p \to K^0\,\Lambda$ and $\pi^- + n \to \Sigma^- K^0$) are summed up according to the number of protons and neutrons per nucleus. The obtained values are multiplied by $A^{2/3}$ to introduce the observed surface-like dependence. The hatched area in Fig. 1 depicts the final result for the K^0 inclusive cross-section for the $\pi^- + A$ reactions including systematic error of the underlying data. Our data (full circles) shows an enhancement of the cross-section for all nuclei.

E-mail address: N.Herrmann@physi.uni-heidelberg.de.

0146-6410/$ – see front matter © 2009 Elsevier B.V. All rights reserved.
doi:10.1016/j.ppnp.2008.12.046

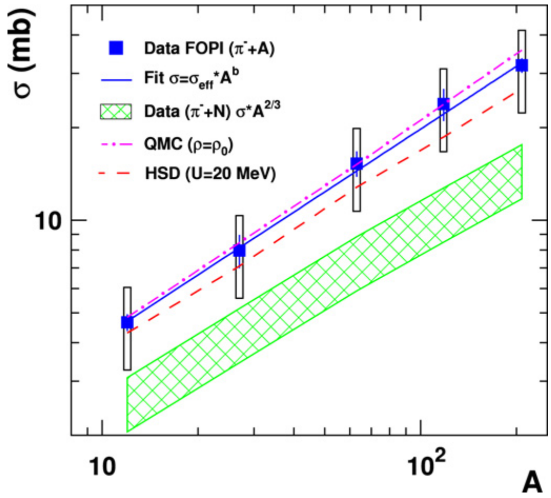

Fig. 1. The K^0 inclusive production cross-section (squares) as a function of the mass number of the target nucleus. The solid line represents the fit with a power law function. The hatched area corresponds to the sum of the cross-sections of the elementary processes scaled according to the transverse size of the target nuclei. QMC model predictions at $\rho = \rho_0$ [7] (dashed dotted line) are scaled with the same prescription, whereas HSD transport model calculations (dashed line) yield absolute predictions.

The data are quantitatively described by the QMC—calculations for finite densities ($\rho = \rho_0$) [7] once the same scaling procedure is applied as for the vacuum cross-section. Within this model the medium effects are acting by influencing the means and widths of intermediate resonances coupling to the kaon. An absolute description of the data can, however, also be obtained within the HSD model [8] introducing a linearly density dependent shift of the mean kaon mass. This effective mass shift is called the kaon potential in the following. Within the HSD approach there is a very limited sensitivity of the inclusive cross-section to the kaon potential, e.g. it is much smaller than the error bars. From this it has to be concluded that most of the enhancement visible in Fig. 1 is due to finite size effects and multi-step processes.

It is, however, possible to extract the KN potential from the data: comparing (in terms of ratio) the K^0 phase space distribution between heavy (Pb, Au) and light (C) targets [9] gives a much better access to the density dependence of the interaction. Due to the repulsive nature of the KN potential, inside a nucleus a K^0 with low momentum will be accelerated and gain kinetic energy while escaping the nucleus. Fig. 2 shows the ratio of the momentum distributions of K^0 (K^+) mesons produced in Pb (Au) to the one produced in C. The measured ratio $(\mathrm{d}\sigma/\mathrm{d}p)_P b/(\mathrm{d}\sigma/\mathrm{d}p)_C$ of K^0 shows similar trends as the one measured for K^+. Above 250 MeV/c both ratios agree quantitatively. This agreement is due to the fact that K^0 (K^+) mesons with high momenta leave the nuclear medium without interaction (i.e. neither Coulomb nor nuclear one) with the surrounding nucleons. Below 200 MeV/c both ratios have the same trend but differ quantitatively. Kaons with low momenta are more sensitive to the nuclear potential but K^+ are influenced by the Coulomb potential in addition. Due to the stronger Coulomb potential in Gold with respect to Carbon nuclei, the ratio of K^+ is suppressed below 250 MeV/c while in the case of K^0, where no Coulomb potential is present, the ratio is suppressed below 170 MeV/c and allows for a direct measurement of the potential in the case of K^0.

To have an estimate of the magnitude of the K^0N potential, transport calculations using the Hadron String Dynamics (HSD) model [8] have been performed. Two cases are shown in Fig. 2: (i) including a linearly density dependent potential of 20 MeV at $\rho = \rho_0$, and (ii) no KN potential. Both versions take into account the K^0 rescattering cross-section. At low momenta, below 170 MeV/c, R(K^0) from HSD without K^0N potential shows a decrease of R(K^0) with increasing momentum. Including the 20 MeV potential, the model exhibits the opposite behavior compared to the one without potential and describes the data quantitatively.

3. Strangeness production in heavy-ion reactions

The kaon potential extracted in π-induced reaction is in good agreement with the value extracted from the flow data of K^+ in heavy-ion collisions [10]. The yields of the kaons and the anti-kaons are less well understood especially since the latter ones couple strongly to the baryons. To address the question of the density dependence of the anti-kaon potential, this coupling needs to be quantitatively understood. Transport models indicate that sub-threshold K^- production results from strangeness exchange reactions $\pi + \mathrm{Y} \leftrightarrow K^- + \mathrm{B}$ whose rate is intimately linked to the hyperon ($\mathrm{Y} = \Lambda, \Sigma$) yield [5,11]. In addition, recent calculations based on the chiral theory predict an important coupling of the K^- to the medium via $\Sigma(1385)$, $\Lambda(1405)$ and $\Lambda(1520)$ resonances [12–15] and reveal, in particular, the importance of the $\Sigma(1385)$ hyperon in sub-threshold K^- production [16]. Strange baryon data are rather scarce in the threshold region motivating the measurement of a comprehensive set of data that includes as many species of strange particles as possible. Λ- and K^0 distributions are reported in [17]. The status of extending the data set to strange resonances is described in the following.

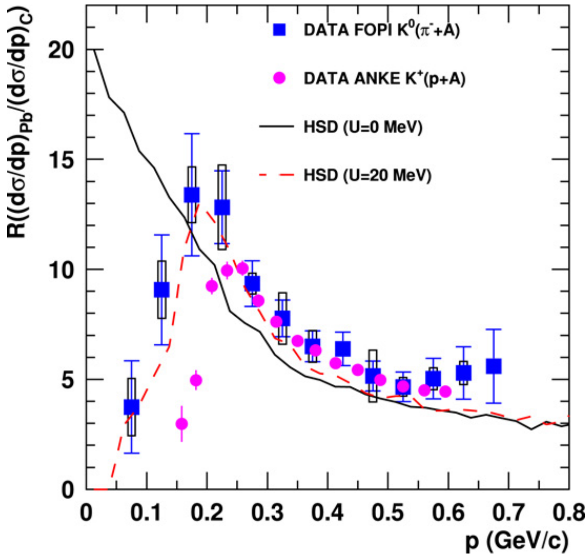

Fig. 2. The ratio of the momentum of K^0 (K^+) produced in Pb (Au) to the one in C. Full squares depict the ratio of K^0 from this experiment (i.e. $\pi^- + A \rightarrow K^0 + X$). The same ratio for K^+ measured in proton-induced reactions is represented by full circles [9]. HSD calculations of R (K^0) without and with K^0 N potential are represented by stars and open crosses, respectively.

3.1. Strange resonance production in heavy-ion reactions

From the high statistics data that has been gathered with FOPI in the last couple of years short lived strange resonances can be reconstructed. Up to now first yields on the $\Sigma^*(1385)$ and the $K^{*0}(892)$ are available from the reaction Al + Al at an incident energy of 1.9 AGeV. Both the resonances are produced well below their production threshold in free NN-collisions that amount to 2.33 GeV and 2.75 GeV, respectively. Since the short life times of the Σ^* and K^{*0} do not allow to disentangle their decay vertex from the collision vertex, the reconstruction consists in correlating particle pairs from the primary vertex. For the reconstruction of the K^{*0}, the 66% decay branch into K^+ and π^- is used. The invariant mass of the particle pair is calculated from the four-momenta of the daughter particles [18]. A total of about $4 \times 10^5 K^+$ are identified with a signal-to-background ratio of about 1.5 from the analysis of 290 million events. The reconstructed K^{*0} are shown in Fig. 3. The combinatorial background is obtained with the event-mixing method. For that purpose, the two decay particles (K^+ and π^-) are taken from two different events which present the same particle multiplicity in the Central Tracking Chamber (CDC). In addition, the two events are aligned to the reaction plane in order to have the same reference system for both particles. The reaction plane is estimated event by event utilizing the transverse momentum procedure detailed in [19]. The shape of the resulting mixed-event background describes the combinatorial background and is indicated by crosses in Fig. 3 (upper panel). The vertical bars of the crosses correspond to the statistical errors. After background subtraction (Fig. 3, lower panel), the remaining peak in the mass spectrum is fitted with a relativistic Breit–Wigner function multiplied with a thermal distribution [20]. Within the width interval (Γ), about 5400 K^{*0} are found for the applied set of cuts in the analysis. The mean mass value and width extracted from the fit are in a good agreement, within statistical errors, with the values reported by the Particle Data Group [21].

A similar analysis was performed for the $\Sigma^{*\pm}$-baryon [22] with the additional complication that the Λ-baryon has to be reconstructed from its weak decay. The corresponding distribution after applying suitable topological selection cuts is shown in the inset of Fig. 3. A total of about 10^5 Λ are reconstructed with a signal-to-background ratio close to 10 from the analysis of 290 million events. $\Sigma^{*\pm}$ are then reconstructed by calculating the invariant mass of these Λ with charged pions after applying a two-sigma mass selection cut around the Λ nominal mass (shown by the dashed lines in the inset of Fig. 3).

The losses due to decay, acceptance and reconstruction efficiency have been corrected by means of GEANT Monte Carlo calculations in order to extract the particle yields. The IQMD model [23] is used as a generator for the underlying heavy-ion event. The $\Sigma^{*\pm}$, K^{*0} and Λ resonances are embedded into those events (one signal per event) with a momentum distribution according to the Siemens–Rasmussen formula [24] which describes an expanding system with a temperature T and a radial expansion velocity β. The choice of the values of these parameters ($T = 90$ MeV, $\beta = 0$ and 0.3) is constrained by transverse momentum spectra [25]. With this input a full simulation of the detector, including resolutions in energy deposition and spatial position, Front-End-Electronics processing and tracking, is performed and the resulting output is subject to the same reconstruction procedure as for the experimental data. Simulated and experimental spectra agree in all relevant quantities. Therefore the reconstruction efficiency is determined by computing the ratio of reconstructed particles in the simulation to those initially embedded into the background events.

The systematic error was evaluated in two steps. First the reconstruction efficiency was estimated for different source parameters, e.g. the radial flow velocity ($\beta = 0$ and $\beta = 0.3$). Then the signals were reconstructed under different sets of conditions on the relevant selection quantities p_{lab}, DCA, d_t, $\Delta\phi$ and p_t (see [22] for details on the Σ^* case). In

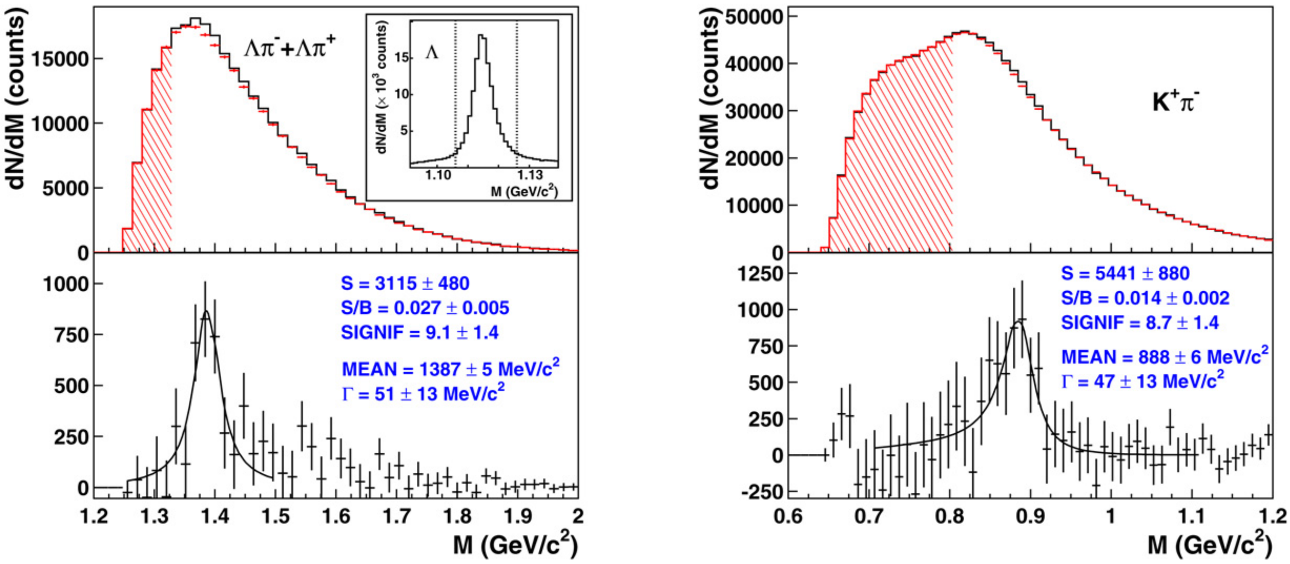

Fig. 3. Invariant mass spectra of $p\pi^-$ pairs (inset, upper left panel) and $\Lambda\pi^{\pm}$ pairs (left panel) and $K^+ - \pi^-$ pairs (right panel). The solid histogram and crosses denote the data and the scaled mixed-event background, respectively (upper panel). The lower panel shows the signal after background subtraction. The following characteristics of the signal are shown: number of counts in the signal (S), signal-to-background ratio (S/B) and significance (SIGNIF). The parameters extracted from the fit to the data (mean mass value (MEAN) and the width (Γ)) are also reported.

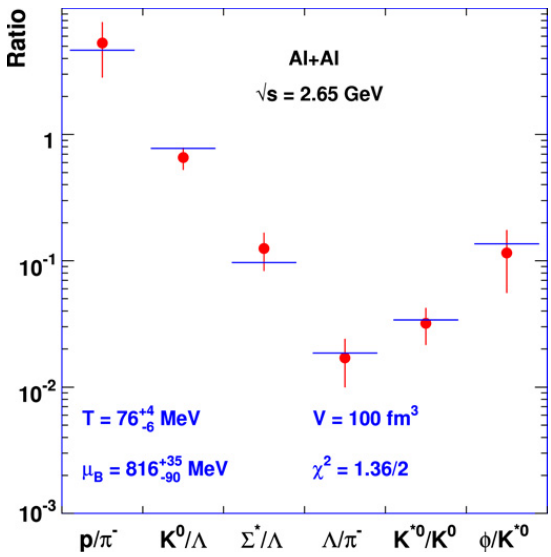

Fig. 4. Comparison of available data from the reaction Al + Al at 1.91 AGeV to thermal model calculations [26]. The data are derived from 4π yields extracted for the most central 315 mb of the reaction. Specific ratios are chosen in order to minimize experimental errors.

order to minimize the statistical errors, the yields of Σ^{*+} and Σ^{*-} are summed and the following ratio is extracted: $\frac{P(\Sigma^{*-}+\Sigma^{*+})}{P(\Lambda+\Sigma^0)} = 0.125 \pm 0.026(\text{stat.}) \pm 0.033(\text{syst.})$. Note that using such a ratio has the additional advantage that the influence of the chosen momentum distribution for the simulated signal is cancelled out to a large extent. A similar procedure was applied for the K^{*0} resonance that was compared for experimental reasons to the K^0 distribution and results in the ratio $\frac{P(K^{*0})}{P(K^0)} = 0.0315 \pm 0.006(\text{stat.}) \pm 0.012(\text{syst.})$.

3.2. Comparison to statistical model calculations

Our experimental data are compared to statistical model predictions for the Al + Al system [26]. The results are shown in Fig. 4 where other particle species such as proton, pion, Λ and K^0 are included.

The statistical model, based on the canonical ensemble, reproduces the ratios with a temperature of 76 MeV and a baryonic chemical potential of $\mu_B = 816$ MeV. These values and the volume necessary to implement the canonical suppression mechanism are obtained from optimizing χ^2 for the first 5 ratios shown in Fig. 4. The theoretical value for the Φ/K^* ratio is a prediction and compared with preliminary data of FOPI from the same reaction. This chemical temperature is in rough agreement with the kinetic temperature of 90 ± 10 MeV derived from the transverse mass spectra. It is surprising

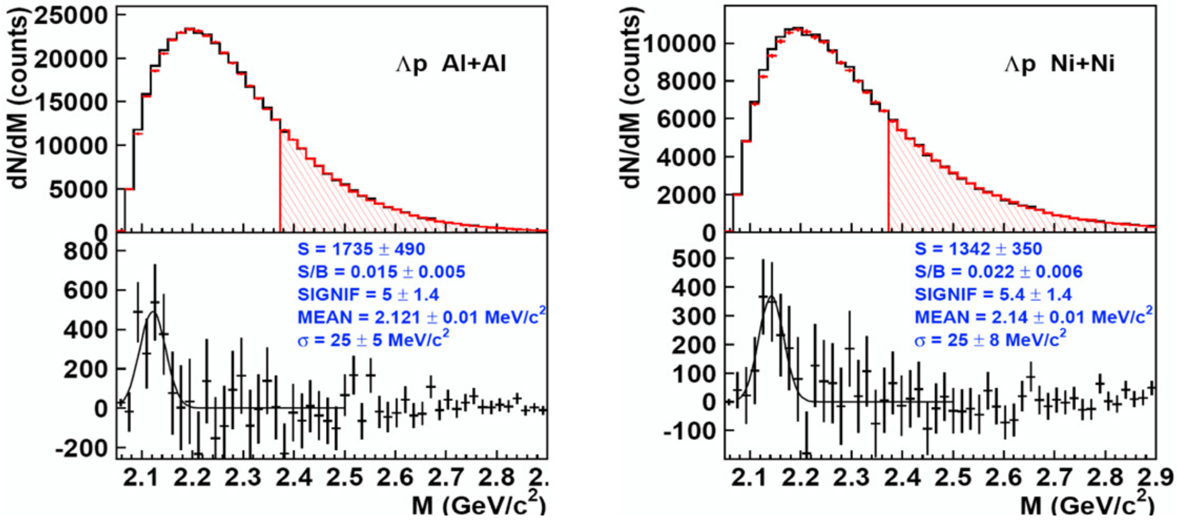

Fig. 5. Invariant mass distribution between Λ-baryons and protons. The solid histogram and crosses denote the data and the scaled mixed-events background, respectively (upper panels). The lower panels show signals after background subtraction. The fitted parameters of Gaussian function (mean value of the mass position (MEAN) and the sigma (σ)) are also reported.

to notice that at this rather low beam energy and for such a small system (Al+Al) even the far-sub-threshold resonances are well reproduced and chemical equilibrium seems to be reached. Even the Φ-meson is well reproduced in the framework of the model calculation employing no general strangeness suppression ($\gamma_s = 1$) but using canonical strangeness suppression within a volume of $V = 100\ \mathrm{fm}^3$. The agreement is by no means trivial since up to now none of the transport codes were able to describe all ratios simultaneously.

3.3. Search for kaonic bound states

The search for deeply bound states was triggered by the theoretical predictions of Akaishi and Yamazaki [27,28] and is actively pursued by many groups. Heavy-ion collisions offer unique possibilities [29] for broad band creation of such states. In our high statistics data samples, besides Λ-deuteron [30] we analyzed Λ-proton correlations. The combinatorial background is reconstructed by using the same technique as was used for the Σ^* measurement [22].

After background subtraction (lower panels of Fig. 5), an excess is found at 2.13 GeV/c^2 for two independent data sets (Al + Al and Ni + Ni reactions) [31]. The significance of the observed structure ($\tilde{5}$) is large enough to stimulate the search for an explanation. Observing in addition that the phase space population is non-uniform and similar to the one of the non-strange clusters triton or ^{3}He, we note that a strange di-baryonic resonance is visible exactly at the ΣN-threshold in elementary particle reactions [33,34]. Whether this so-called H1$^+$ resonance is being produced in heavy-ion collisions and can reproduce the data consistently is a matter of ongoing investigations. It is worth noting that the invariant mass spectra do not show any evidence of the signal in the range between 2.2 and 2.3 GeV/c^2 where a (ppK$^-$)-candidate is found by the FINUDA collaboration [32].

4. Conclusion

New data have been presented for elucidating the properties of strange particle in dense baryonic matter. While the picture of kaons carrying the anti-strange quark is quite well established pointing to a linearly density dependent mean field potential of depth U = 20 MeV at normal nuclear matter density, the situation for the particles carrying the strange quark is far less known. Strange baryons play an important role and appear to be formed with statistical yields even for a system as small as Al+Al and far below their NN production threshold. Indications exist that even di-baryonic strange states are populated, opening new possibilities to study hadronic states in the hadronic environment of a heavy-ion collision.

Acknowledgments

This work was supported by the German BMBF under Contract No. 06HD190I, by the Korea Science and Engineering Foundation (KOSEF) under Grant No. F01-2006-000-10035-0, by the mutual agreement between GSI and IN2P3/CEA, by the Hungarian OTKA under Grant No. 47168, within the Framework of the WTZ program (Project RUS 02/021), by DAAD (PPP D/03/44611), and by DFG (Projekt 446-KOR-113/76/04).We have also received support from the European Commission under the 6th Framework Program under the Integrated Infrastructure on: Strongly Interacting Matter (Hadron Physics), Contract No. RII3-CT-2004-506078.

References

[1] G.E. Brown, et al., Nuclear Phys. A 567 (1994) 937.
[2] W. Weise, Nuclear Phys. A 610 (1996) 35c.
[3] G.Q. Li, et al., Nuclear Phys. A 625 (1997) 372.
[4] D.B. Kaplan, A.E. Nelson, Phys. Lett. B 175 (1986) 57.
[5] C. Fuchs, Prog. Part. Nucl. Phys. 56 (2006) 1.
[6] M.L. Benabderahmane, et al., [FOPI Collaboration]. arXiv:0807.3361[nucl-ex].
[7] K. Tsushima, et al., Phys. Rev. C 62 (2000) 064904.
[8] W. Cassing, et al., Phys. Rep. 308 (1999) 65.
[9] M. Buescher, et al., [ANKE Collaboration], Eur. Phys. J. A 22 (2004) 301.
[10] P. Crochet, et al., [FOPI collaboration], Phys. Lett. B 486 (2000) 6.
[11] C. Hartnack, H. Oeschler, J. Aichelin, Phys. Rev. Lett. 90 (2003) 102302.
[12] W. Cassing, L. Tolos, E.L. Bratkovskaya, A. Ramos, Nuclear Phys. A 727 (2003) 59.
[13] M.F.M. Lutz, C.L. Korpa, Nuclear Phys. A 700 (2002) 309.
[14] J. Schaffner-Bielich, V. Koch, M. Effenberger, Nuclear Phys. A 669 (2000) 153.
[15] L. Tolos, A. Ramos, A. Polls, T.T.S. Kuo, Nuclear Phys. A 690 (2001) 547.
[16] M.F.M. Lutz, Prog. Part. Nucl. Phys. 53 (2004) 125.
[17] M. Merschmeyer, et al., [FOPI Collaboration], Phys. Rev. C 76 (2007) 024906.
[18] P. Velten, Master thesis, Université Louis Pasteur de Strasbourg (2007) (unpublished).
[19] P. Danielewicz, G. Odyniec, Phys. Lett. B 157 (1985) 146.
[20] J. Adams, et al., [STAR Collaboration], Phys. Rev. Lett. 97 (2006) 132301.
[21] W.-M. Yao, et al., J. Phys. G 33 (2006) 1.
[22] X. Lopez, et al., [FOPI Collaboration], Phys. Rev. C 76 (2007) 052203.
[23] C. Hartnack, et al., Eur. Phys. J. A 1 (1998) 151.
[24] P.J. Siemens, J.O. Rasmussen, Phys. Rev. Lett. 42 (1979) 880.
[25] B. Hong, et al., [FOPI Collaboration], Phys. Rev. C 57 (1998) 244; Phys. Rev. C 58 (1998) 603.
[26] A. Andronic, P. Braun-Munzinger, J. Stachel, Nuclear Phys. A 772 (2006) 167.
[27] Y. Akaishi, T. Yamazaki, Phys. Rev. C 65 (2002) 044005.
[28] T. Yamazaki, A. Doté, Y. Akaishi, Phys. Lett. B 587 (2004) 167.
[29] T. Yamazaki, et al., Nuclear Phys. A 738 (2004) 168.
[30] N. Herrmann, [FOPI collaboration], Proceedings of EXA05 Conference, Österreichische Akademie der Wissenschaften, ISBN: 3-7001-3616-1, 2005, p. 73.
[31] X. Lopez, [FOPI Collaboration], J. Phys. G 35 (2008) 044020.
[32] M. Agnello, et al., Phys. Rev. Lett. 94 (2005) 212303.
[33] O. Braun, et al., Nucl. Phys. B 124 (1977) 45.
[34] C. Pigeot, et al., Nucl. Phys. B 249 (1985) 172.